J Mater Sci (2007) 42:9276–9283
DOI 10.1007/s10853-007-1864-7

Influence of temperature on fracture initiation in PET and PA66 fibres under cyclic loading

Christophe Le Clerc · Bernard Monasse · Anthony Roland Bunsell

Received: 16 March 2007 / Accepted: 18 May 2007 / Published online: 27 July 2007

Abstract The fatigue of single thermoplastic fibres has been well documented to occur in a reproducible manner when they are subjected to certain cyclic loading conditions. The fatigue fracture morphologies of these fibres are very distinctive and differ markedly from other types of failure. This type of behaviour, which is clearly seen with the unambiguous tests on single fibres, must reflect behaviour of fibres in more complex structures which are subjected to cyclic loading. Only limited numbers of reports have, however, shown similar fracture morphologies with fibres extracted from fibre bundles embedded in a matrix material such as rubber. Usually the fractured ends of fibres taken from structures are seen to be shorter than those obtained in single fibre tests and also they show more complex and confused crack growth. The present study reveals that the low thermal conductivity of the fibres, exacerbated when they are embedded in a rubber matrix, leads to very high temperature rises, which is not the case in single fibre tests and under these conditions, crack initiation occurs across the fibre section instead of being restricted to the near surface region. Tests on single fibres at temperatures up to and beyond the glass transition temperature have shown how the fracture morphologies become modified. The fatigue process has been seen to become generalised throughout the fibre and failure occurs due to the coalescence of several cracks, some of which are initiated in the core of the fibre. In all cases, the cracks can be seen to have been initiated by solid inclusions in the fibres.

C. Le Clerc · B. Monasse · A. R. Bunsell (✉)
Centre des Matériaux, Ecole des Mines de Paris, BP 87, 91003 Evry Cedex, France
e-mail: anthony.bunsell@mat.ensmp.fr

Introduction

The fatigue failure of thermoplastic fibres occurs under cyclic tensile loading conditions considerably lower than those load levels which produce tensile failure and fatigue leads to more rapid failure than observed in creep [1–4]. It has long been known that single fibres subjected to fatigue loading conditions fail with very distinctive fracture morphologies involving crack initiation near the fibre surface and crack propagation along the fibre, at a small angle to the axial direction so that the crack penetrates into the fibre, gradually reducing its load bearing cross section [5]. In the case of both polyamide 6 and 66 fibres the final failure stage is that of the tensile failure of the reduced cross section whereas polyethylene terephthalate and polyethylene napthalate fibres [6] fail by creep at a point behind the tip of the fatigue crack. The fatigue cracks are initiated at weak points in the fibre, which for single fibres tested at room temperature is at the interface between the skin and the core, about 1 μm under the fibre surface. Recent studies have revealed that under these conditions crack initiation is triggered by the presence of small, hard inclusions deliberately included in the polymer before drawing as catalysts or carriers for antioxidant or flame retardant products [7]. In some rare cases crack initiation has been observed to have been initiated by particles within the body of the fibre leading to cone and crater complimentary broken ends in fatigued fibres [8].

Fatigue failure seen in single fibre tests occurs when the fibre is subjected to cyclic loading of a sufficiently high amplitude. A necessary criterion however for fatigue failure is that the minimum load must be lower than a certain threshold. Buckling is not involved in the failure as the minimum load can be up to about 10% of failure load, so that the fibre never buckles. Raising the cyclic loading

pattern to increasingly higher loads, so that the minimum load increases produces an increase in lifetime and finally suppression of the fatigue phenomenon. The molecular processes involved in the fatigue process have been the subject of several publications [9, 10].

The mechanisms of fatigue failure of fibres in bundles and embedded in a rubber matrix have been difficult to determine however it is clear that the fatigue process seen with individual fibres, under simple and unambiguous testing conditions, must occur in fibres making up a bundle or tow subjected to cyclic tensile loading. Such a fatigue process could be of importance in determining lifetimes of technical structure, such as cables, cords, belting and tyres however the distinctive fracture morphologies found with fatigued single fibres have been little reported in the literature. This lack of observed fracture morphologies has been surprising, even given the difficulties of identifying the original fibre breaks in a large population of fibres.

Recently obtained results on single PET fibres tested at temperature and also yarns tested at room temperature, at 50 Hz, have revealed both the long fractures, typical of fatigue failure at room temperature and also more truncated breaks involving several cracks [7]. The truncated breaks are similar to those found with broken fibres removed from fibre structures and fibres which had been embedded in rubber and subjected to cyclic loading. Tests on single fibres revealed that as the temperature was raised to the glass transition temperature (T_g) increasing numbers of the truncated fatigue breaks were observed. Around T_g a majority of truncated breaks were found although some typical of room temperature fatigue were also seen. Above T_g only the truncated fatigue breaks were observed. The yarns tested at room temperature were found to increase in temperature as the heat generated by fibres inside the yarn could not easily be dissipated and temperature rises up to the region of the T_g were measured. It is clear from these observations that the appearance of fatigue failures changes as the temperature is increased, particularly beyond T_g.

Crack initiation has been seen, most clearly in fatigue but possibly also in other types of failure to have been initiated by the presence of inclusions, submicron in size and placed in the polymer as catalysts or carriers for antioxidant or flame retardants.

Experimental details

Material

The polyester (PET) used for this study was a technical yarn with high modulus and low shrinkage (HMLS). The PET fibres had a median diameter of 18.5 μm (±0.8 μm), an initial modulus of 14 GPa (±0.5 GPa), a tensile strength of 1 GPa (±0.05 GPa) and elongation at tensile break of 12% (±3%) at 20 °C. The polyamide 66 fibres were also of a type used in technical yarns. The polyamide 66 fibres had a median diameter of 27.1 μm (±0.8 μm), an initial modulus of 5 GPa (±0.5 GPa), a tensile strength of 1 GPa (±0.03 GPa) and elongation at tensile break of 20% (±1%) at 20 °C. Fibres with these mechanical properties are obtained by high speed spinning so that the molecular orientation and the crystallinity are very high; the degree of crystallinity is about 50% and the birefringence is 0.221.

Mechanical tests

All tensile and fatigue tests were conducted on machines originally designed by Bunsell et al. [11] which are described in detail elsewhere. The fibre is held between two clamps, one connected to a sensitive transducer mounted on a screw thread connected to a motor controlling the crosshead, the other is fixed, for creep or tensile tests, or connected to a vibrator for fatigue tests. The load imposed on the fibre is controlled by a servomechanism comparing the measured load to that required and if necessary, adjusting the cross-head so as to achieve the chosen load level. A tensile test consists of a controlled increase of load, at a constant chosen speed, until failure; a creep test consists however of an initial rapid load increase which then slows when within 10% of the desired load so as to avoid overshooting. In a creep test, the load is maintained constant until failure, with automatic compensation for the elongation which occurs during the test. Fatigue tests are similar to creep tests in that the loading conditions are maintained constant despite any elongation due to creep or plastic deformation, however a cyclic load is superimposed on a steady load. In a load controlled experiment, the maximum load is determined as the sum of the steady load and the amplitude (half crest to trough) of the cyclic load. This value is compared by the servo system to the required maximum load. A LVDT transducer monitors the displacement of the crosshead during a test. Fatigue tests can be chosen to be controlled either as a function of maximum load or displacement.

The main characteristics of this system are very precise load control, with an accuracy of 0.1 g (9.81×10^{-4} N) between 0 and 100 g (9.81×10^{-1} N), a displacement with a precision of 1 μm up to 20 mm. In this study the vibrator was used at 50 Hz with a maximum displacement of ±3 mm. Displacement of the vibrator is monitored by a capacitive transducer with a resolution of ±1 μm. The gauge length used was 30 or 50 mm, depending on the experimental conditions; in the case for which a large elongation was required a gauge length of 30 mm was used. Monitoring the cyclic load and deformation allows the energy dissipated each cycle to be measured throughout

the test. The equipment is described in greater detail elsewhere (7).

In order to investigate the behaviour of the fibres at temperature, a cylindrical heater was added to the machine; it enabled experiments from 20 to 300 °C to be carried out. The specimen was heated evenly over its whole length and the grips were introduced into the heating chamber. Hot jaws were chosen to avoid thermal gradients along fibre. An air cooling system was added to the grip linked to the piezoelectric transducer to avoid signal drift. Furthermore, to refine displacement data during fatigue test, a capacitive captor was added between the vibrator and grip. The testing apparatus is shown in [9].

Tensile tests were carried out at an elongation rate of 50%/min; so that, the whole test lasted about 20 s. More than 30 tests were performed at room temperature so as to determine the median properties of the fibres. At each other temperature at least four tests were carried out. The creep tests and fatigue tests were defined relative to a reference load which was the median breaking load of the fibre at the tested temperature and normalised to the fibre diameter. The stress–strain or strain–time curves were obtained using ATS software.

Scanning electron microscopy (SEM) observations

Fracture morphologies of broken fibres were observed with a Zeiss scanning electron microscope (Gemini 982). This microscope was equipped with a field effect gun which allowed working at low electron beam voltages which, in this study, were usually 2 kV. This ensured that the specimens were not damaged by the electron beam and gave improved images of the fibre surfaces. The fibres were coated with a 3 nm layer of gold/palladium to avoid charging problems.

X-ray analyses were also carried out to determine the nature of the inclusions. Energy dispersive spectrometry was used with a working distance of 10 mm and an accelerating voltage of 10 kV.

Transmission optical microscopy

Transmission optical microscopy was possible on the as received or tested specimens because of the transparency of the polyester or polyamide 66 fibres. Two microscopes were used in this study: a Reichert and a Leica equipped with a Nikon numerical camera used with the Leica im1000 software. Several objectives with magnifications, from 20 to 100×, were used.

Fibres were held in between a slide and a cover glass and immersed in a mineral oil with a refractive index of 1.515, close to that of the polymer refractive index, in order to avoid optical reflection and refraction at the curved surface of the fibre. In the best optical conditions, the optical resolution was better than 0.4 μm. As thermoplastic fibres are highly oriented, they present a high birefringence and polarised light could was able to emphasise any local variation of birefringence of the material corresponding to a variation in orientation.

Microtomy

Microtome sectioning was carried out on fibres with an Ultracut Microtome from Leica. Fibres were embedded in a resin between two polyester films. Microtoming was performed at room temperature with a 35° diamond knife perpendicularly to the fibre axis and with a section thickness between 1 and 1.5 μm. These sections were collected from pure water using the capillarity induced with a whisker and then observed under the microscope.

Results

Tensile behaviour

The effect of temperature on the stress-strain curves of both PET and PA66 fibres can be seen in Figs. 1 and 2. These effects on PET fibres are described in greater detail elsewhere [9] and broadly similar effects are seen with the more deformable PA66 fibres. The failure stress of both types of fibre falls in a linear manner as a function of temperature and is shown in Figs. 3 and 4. The fall in strength at the highest temperatures, well above the T_{gs} of both fibres, whilst significant, is not great. This is attributed to the high crystallinity and molecular alignment of both types of fibres which restricts movement. Figures 3 and 4

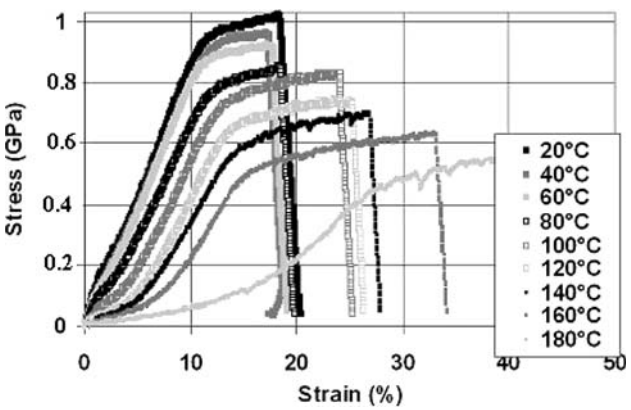

Fig. 1 The effects of temperature on the tensile behaviour of PET fibres

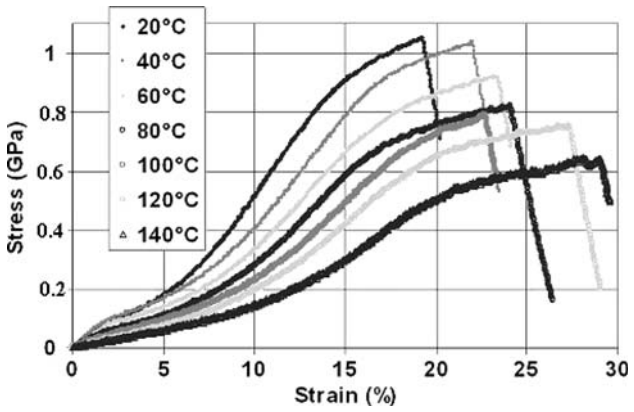

Fig. 2 The effects of temperature on the tensile behaviour of PA66 fibres

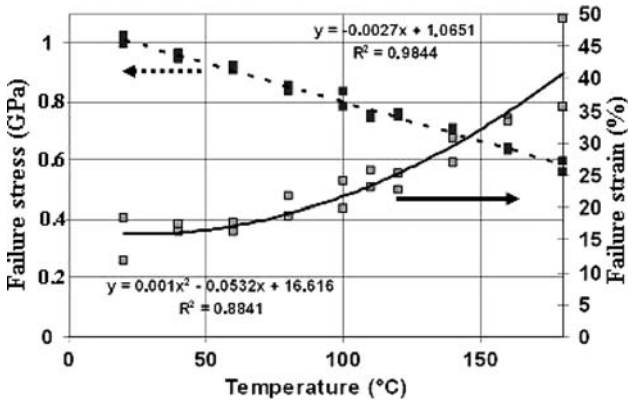

Fig. 3 Failure stress and strain as a function of temperature for the PET fibres

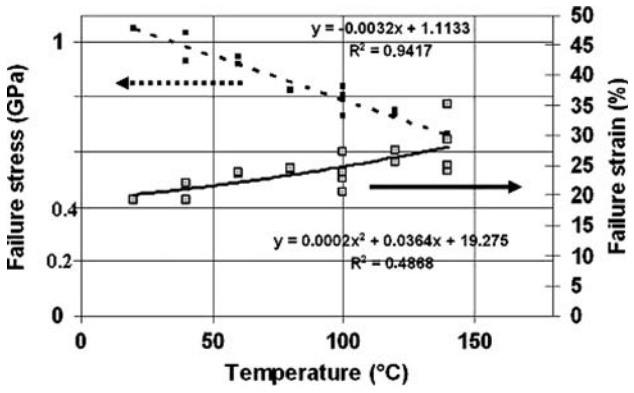

Fig. 4 Failure stress and strain as a function of temperature for the PA66 fibres

also show that the strains to failure of the fibres do not vary linearly with temperature.

Simple tensile failure of both types of fibre at room temperature results in very similar fracture morphologies, which have been widely reported in the literature [1–5, 7, 12, 13]. This generally involves initiation at or near the surface and slow crack growth normal to the fibre axis direction. This leads to plastic deformation ahead of the crack and crack opening. When the load bearing cross section is sufficiently reduced, it fails rapidly. This results in two similar distinctive broken ends showing an inclined, bevelled region resulting from the slow crack growth stage of failure, followed by a fracture surface normal to the fibre axis resulting from the final rapid failure stage. Examples of these breaks can be seen in the papers to which reference is made above. Occasionally several cracks will initiate in the same region and this can lead to step like breaks. Figure 5 shows one end of a broken PA66 fibre tested in tension at room temperature, together with a close up view. This image reveals that the crack was initiated just under the surface of the fibre rather than by some irregularity at the surface, as is often supposed by analogy to failure in metals and brittle solids.

Failure at high temperatures, particularly above T_g leads to less sharp fracture morphologies and more microcracking, as can be seen from Fig. 6 for PET fibres.

Creep failure morphologies of both fibres resemble very closely the simple tensile fracture morphologies described above and elsewhere [10]. Failure at higher temperatures is again seen to encourage multiple points of fracture initiation and above T_g voids were seen to have occurred during creep, as shown in Fig. 7.

Fatigue failure initiation

The fatigue failure of PET and PA66 fibres at room temperature is well documented [1–7]. The fracture morphologies of fibres broken in fatigue are unmistakably different from those broken in simple tension or creep. They show two complementary ends, one of which consists of a long tongue of material whilst the other shows a concave impression from where the tongue has been removed. Figure 8 shows the tongues obtained at room temperature with a PET fibre and a PA66 (nylon) fibre. The crack initiation, in both cases has occurred near the surface and propagation has been along the fibre at a small angle to the axis direction.

The angle of penetration is greater with the PA66 fibre leading to a more rapid reduction in load bearing cross-section than with the PET fibre. The result is that the fracture tongues are much longer with the PET fibres and ultimate failure occurs by creep behind the fatigue crack tip. The final stage of fracture for the PA66 fibre is by simple tensile failure at the tip of the fatigue crack. The loading criteria for this type of failure are described in the literature and will not be discussed in detail in this paper, however it is clear that the minimum load experienced during load cycling is an important criterion in determining fatigue lifetimes and whether or not the fibre will fail by a

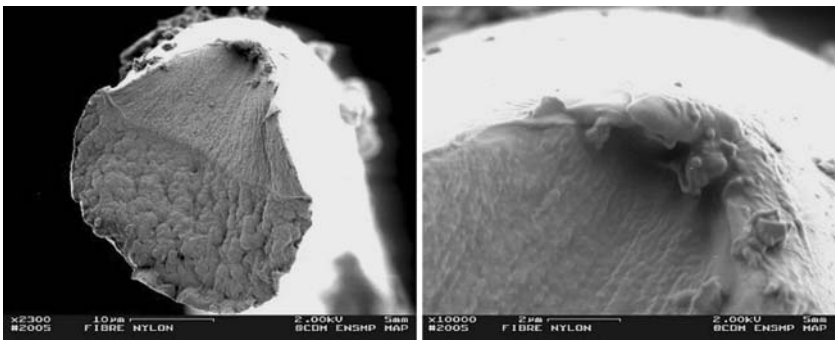

Fig. 5 A broken end of a PA66 fibre tested at room temperature. The crack can be seen to have initiated just under the fibre surface

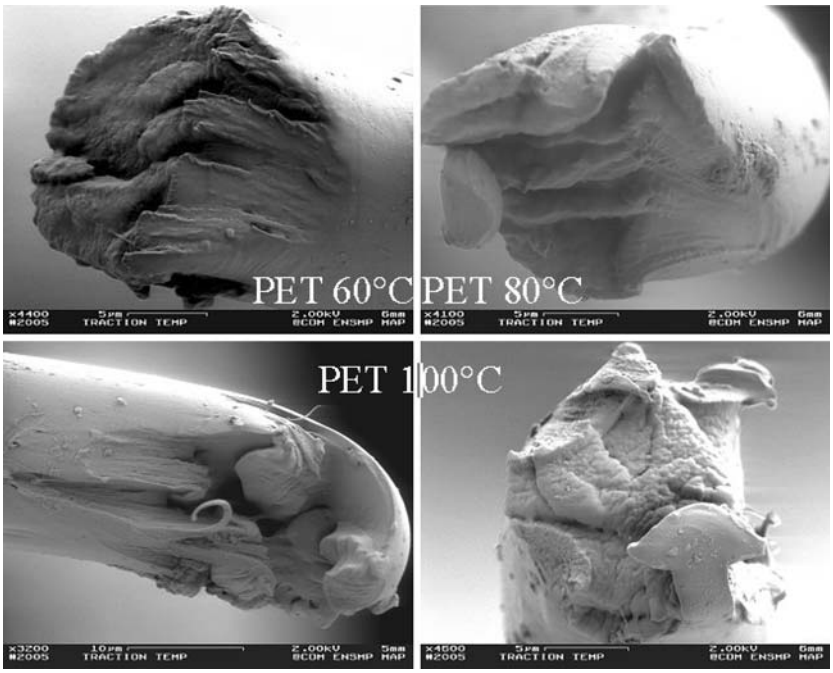

Fig. 6 Fracture morphologies of PET fibres broken around the T_g

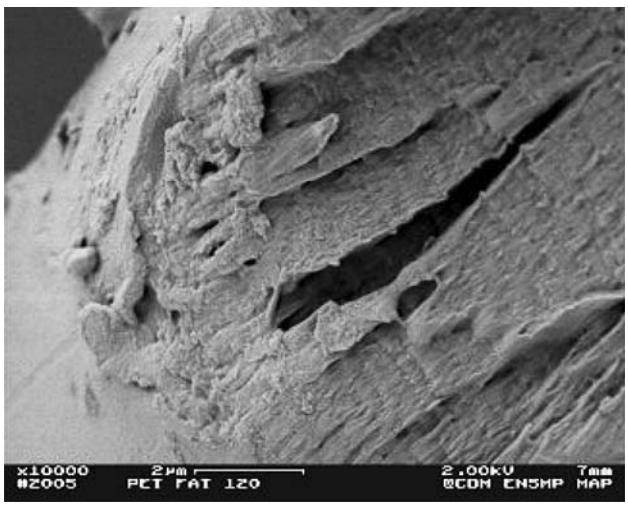

Fig. 7 Voids seen on the creep fracture surface of a PET fibre tested at 80% of breaking load at 120 °C

fatigue process [3, 12]. This is related to the amount of energy dissipated during a load cycle by the fibre at low loads. The lower the minimum load the greater is the energy dissipated. Raising the minimum cyclic load can be seen, from Figs. 9 and 10, for both types of fibres, to decrease the dissipated energy more dramatically than any change in maximum cyclic load.

Fatigue fracture initiation at room temperature has been shown to occur, most commonly, between a surface skin and the core of both PET and PA66 fibres at points where there are small hard inclusions. As the temperature is raised to 80 °C the number of these types of failures reduces to about 25% of specimens tested and the tongue of material, which reflects the fatigue crack length, becomes shorter. At this temperature however approximately 75% of failures are of a truncated complex fatigue fracture type, as shown in Fig. 11 for PET fibres and Fig. 12 for PA66 fibres.

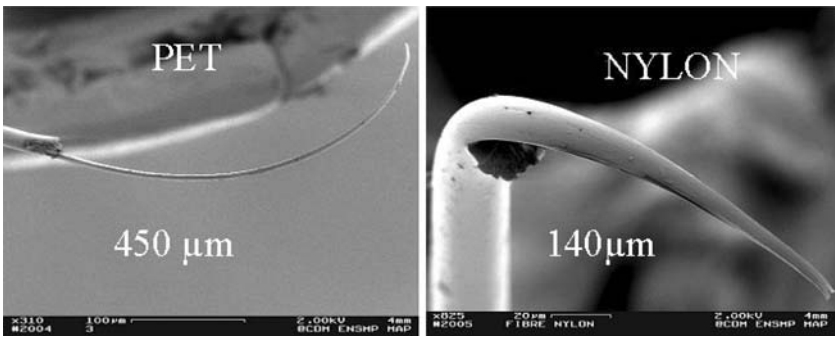

Fig. 8 One half of fatigued PET fibre and one of a fatigued PA66 fibre showing the lengths of the tongues. The lengths of the tongues, for both fibres, are indicated on the figures

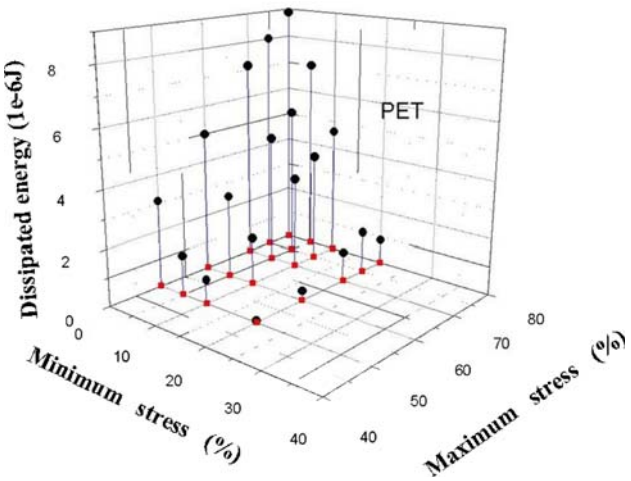

Fig. 9 Energy dissipated during cyclic loading of PET fibres as a function of changes in minimum cyclic load and maximum cyclic load

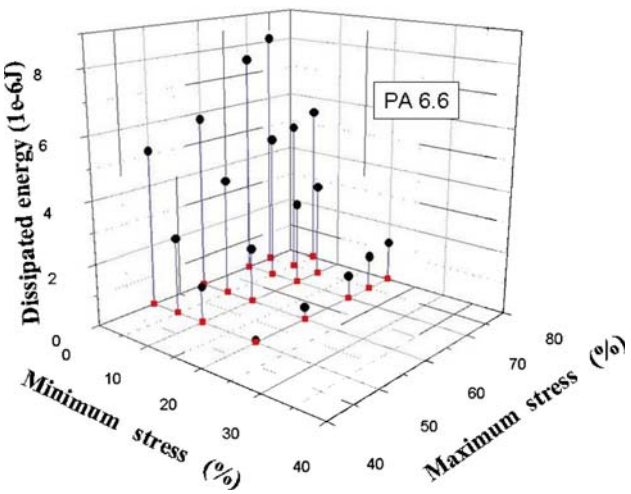

Fig. 10 Energy dissipated during cyclic loading of PA66 fibres as a function of changes in minimum cyclic load and maximum cyclic load

As reported elsewhere the tensile fractures, room temperature fatigue morphologies and the truncated fatigue fractures have been observed to occur together in PET yarns which have been cycled at 50 Hz at room temperature [9]. The temperature of the yarns has been measured as increasing above the ambient temperature due to poor heat dissipation and to reach 80 °C and above.

The observation of the points of initiation of truncated fatigue cracks at 80 °C and higher is difficult because of the complexity of the fractures, however Fig. 13 shows a transmission optical micrograph of a failed PET fibre revealing several inclusions, which have been circled to help identification, associated with the break. Similar observations have been made with PA66 fibres tested at and above 80 °C.

Figure 14 shows a series of microtomed sections through a truncated fatigue fracture of a PET fibre broken at 120 °C. The images have been taken in polarised light. The sections are shown in reverse order of microtoming so as to show more readily the evolution of the complex break. Several breaks are ringed and it can be seen that one of the points of damage occurs in the region where fatigue failure is initiated at room temperature, near the fibre surface. However other cracks can be seen to form within the fibre. These are circled with continuous rings and it can be seen that they do not extend to the surface of the fibre. Failure occurs when several of these breaks coalesce. The bottom three sections are sections have been obtained in non polarised light and reveal the presence of inclusions which are associated with the presence of the internal cracks.

Discussion

The initiation of cracks in PET and PA66 fibres can be seen to be greatly influenced both by the macroscopic make up of the fibre and the presence of sub-micron inclusions. The skin–core interface together with internal residual stresses, originally revealed by Raman Spectroscopy [14] represent a weak interface just under the fibre surface at a depth of less than one micron. This skin can be seen on some fracture morphologies, observed by scanning electron microscopy and by transmission optical microscopy [9].

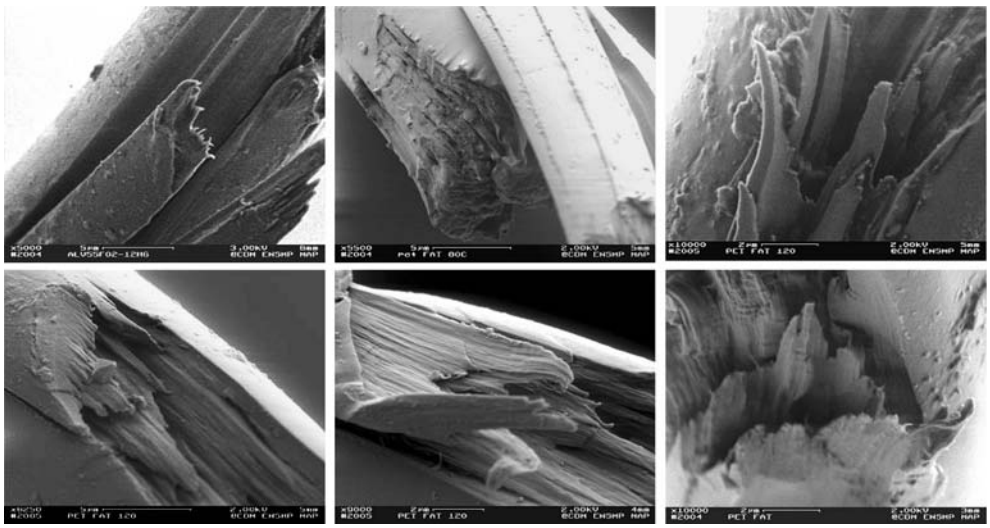

Fig. 11 Truncated fatigue fractures obtained with PET fibres tested at 80 °C

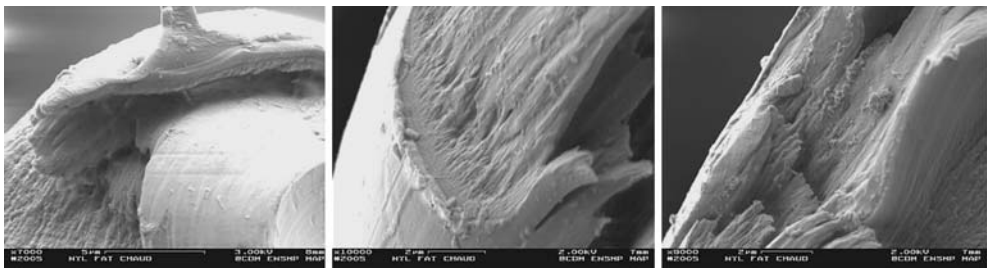

Fig. 12 Truncated fatigue fractures obtained with PA66 fibres tested at 80 °C

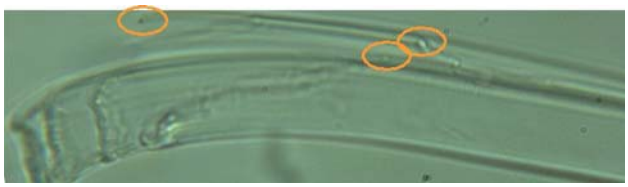

Fig. 13 Optical micrograph of a truncated fatigue fracture of a PET fibre, tested at 80 °C, revealing several inclusions associated with the break

At room temperature the presence of a small inclusion at this skin–core interface creates a weak point in the fibre which can initiate failure. Although this mechanism of crack initiation was first identified in fatigue tests, it can be seen from Fig. 5 that tensile failure initiation can also be associated with the same region at less than one micron under the fibre surface.

Fibres subjected, at room temperature, to cyclic loading conditions, which lead to fatigue, fail by a distinctive fracture process. After initiation, it is most likely that shear stresses at the crack tip, combined with the anisotropy of the drawn fibres, lead to the gradual penetration of the fatigue crack into the fibre and its eventual failure. At room temperature these breaks are initiated at inclusions situated at the skin–core interface. Exceptionally, at room temperature, fatigue breaks may be initiated at points within the body of the fibre and lead to distinctive conical breaks [8]. In these latter breaks the size of particles initiating the failure was seen to be around one micron which is at the upper limit of the size range reported by Le Clerc et al. [7]. It is interesting to note that these conical cracks do not lead to such long fatigue failure morphologies as when the crack is initiated near the fibre surface. Energy dissipation falls as maximum cyclic load falls but if the minimum load remains low the dissipation remains significant. This suggests that there is no load threshold level for the maximum cyclic load below which the fatigue process is arrested.

As the temperature of the fibre is increased, either in single fibre tests by increasing the temperature of the surroundings or through internal heating of the fibres in a bundle or cord, the appearance of the fatigue break changes. Up to around the T_g of both types of fibre the room temperature type fatigue fracture morphology can be observed but as the temperature increases there are increasing numbers of truncated fatigue breaks. Above T_g the truncated fatigue breaks become the norm. The processes involved are an extension of the mechanisms seen at room temperature as initial damage is seen still at the fibre–core interface but the presence of particles within the body of the fibre initiates crack propagation. It has been seen that these internal cracks do not necessarily exit at the fibre surface but clearly weaken the fibre. That the cracks do not

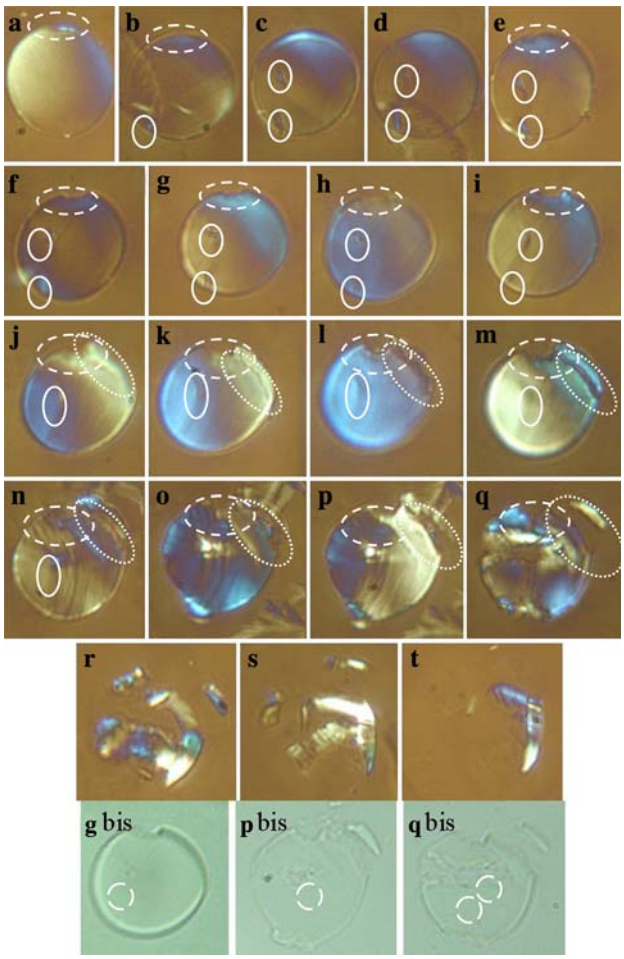

Fig. 14 Microtomed sections through the truncated fatigue break of a PET fibre tested at 120 °C and observed in polarised light. The bottom three images have been obtained in non-polarised light

reach the fibre surface means that there is no significant shear stress generated at the crack tip. This combined with the number of cracks in the same section of the fibre means that propagation along the fibre is limited. As has been demonstrated, it is likely that several independent cracks can be initiated within any given length of fibre. Eventually these cracks coalesce and the complex truncated fatigue break occurs.

It seems likely that the increased temperature reduces transversal bonds between microfibils making up the fibres so that the weak interface, provided by the skin–core boundary, is no longer unique and failure can be initiated throughout the body of the fibre encouraged by the presence of inclusions.

The truncated fatigue breaks observed in this study resemble exactly the fibre breaks taken from yarn embedded in a rubber matrix subjected to a disk fatigue test, as reported by Yabuki et al. [15], Winkler [16] and Naskar et al. [17]. It is clear that in this type of test, the fibres are subjected to large temperature increases due to internal damping and the poor heat transfer properties of the fibres and the rubber. The appearance of the fatigue breaks is then that of the truncated fatigue morphologies rather than those observed with single fibres tested at room temperature, for which heat exchange with the surrounding environment was has been calculated to be of the order of only several degrees Celsius. The observations of the initiation of cracks at inclusions in the fibres clearly explains the origin of the failure process and may suggest ways in which the fatigue properties of these fibres and their composites can be improved.

Acknowledgments The authors wish to express their thanks to Y. Favry and A. Piant both for their technical assistance and their contributions to the discussion.

References

1. Bunsell AR, Hearle JWS (1974) J Appl Polym Sci 18:267
2. Oudet C, Bunsell AR, Hagege R, Sotton M (1984) J Appl Polym Sci 29:4363
3. Oudet C, Bunsell AR (1987) 22:4292
4. Veve JC, Bunsell AR, Baillie C (1987) Kautschuk + Gummi Kunststoffe 40:941
5. Bunsell AR, Hearle JWS (1971) J Mater Sci 6:1303
6. Lechat C, Bunsell AR, Davies P, Piant A (2006) J Mater Sci 41:1745
7. Le Clerc C, Bunsell AR, Piant A, Monasse B (2006) J Mater Sci 4:6830
8. Herrera Ramirez JM, Bunsell AR (2005) J Mater Sci Lett 40:1269
9. Le Clerc C, Bunsell AR, Piant A (2006) J Mater Sci 41:7509
10. Bunsell AR, Oudet Ch, Veve J-Ch (1986) J Mater Sci Lett 5:1101
11. Bunsell AR, Hearle JWS, Hunter RD (1971) J Phy E: Sci Instrum 4:868
12. Hearle JWS, Lomas B, Cooke WD (2000) Atlas of fibre fracture and damage to textiles, 2nd edn. CRC Press
13. Marcellan A, Bunsell AR, Piques R, Colomban Ph (2003) J Mater Sci 38:2117
14. Marcellan A, Colomban Ph, Bunsell AR (2004) J Raman Spectroscopy 35:308
15. Yabuki K, Iwasaki M, Aoki Y (1986) Text Res J 56:43
16. Winkler EM (1991) Text Res J 61:441
17. Naskar AK, Mukherjee AK, Mukhopadhyay R (2004) Polym Degrad Stab 83:173